One-dimensional $CdS@Cd_{0.5}Zn_{0.5}S@ZnS-Ni(OH)_2$ nano-hybrids with epitaxial heterointerfaces and spatially separated photo-redox sites enabling highly-efficient visible-light-driven H_2 evolution

Qinqin Ruan,[a,†] Xiaowei Ma,[a,b,†] Yanyan Li,*[a] Jiakun Wu,[a] Zhiyang Wang,[c] Yanling Geng,[a] Wenjing Wang,[a] Haifeng Lin*[a] and Lei Wang[a]

[a] *Taishan Scholar Advantage and Characteristic Discipline Team of Eco Chemical Process and Technology, Key Laboratory of Eco-chemical Engineering, College of Chemistry and Molecular Engineering, Qingdao University of Science and Technology, Qingdao 266042, P. R. China*

[b] *College of Materials Science and Engineering, Liaocheng University, No. 1 Hunan Road, Liaocheng 252059, P. R. China*

[c] *Key Laboratory of Design and Assembly of Functional Nanostructures, Fujian Institute of Research on the Structure of Matter, Chinese Academy of Sciences, Fujian 350002, P. R. China*

† These authors contributed equally to this work.

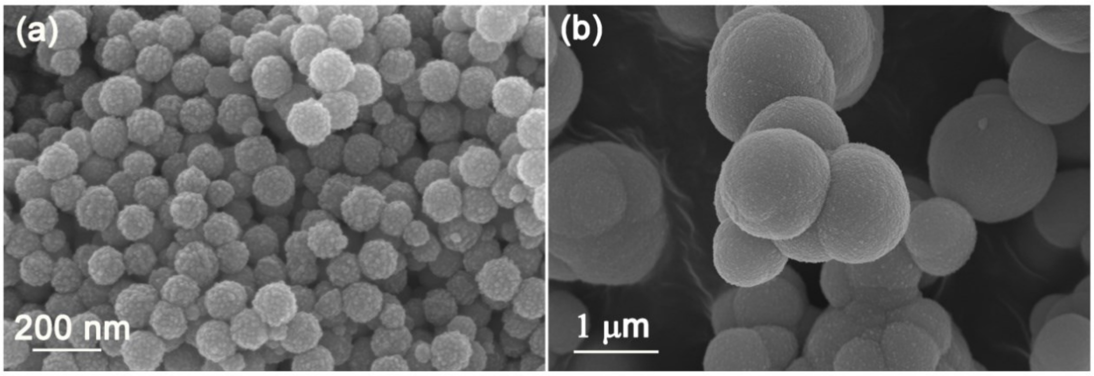

Fig. S1. SEM images of (a) $CZ_{0.5}S$ and (b) ZnS assembled nano-spheres.

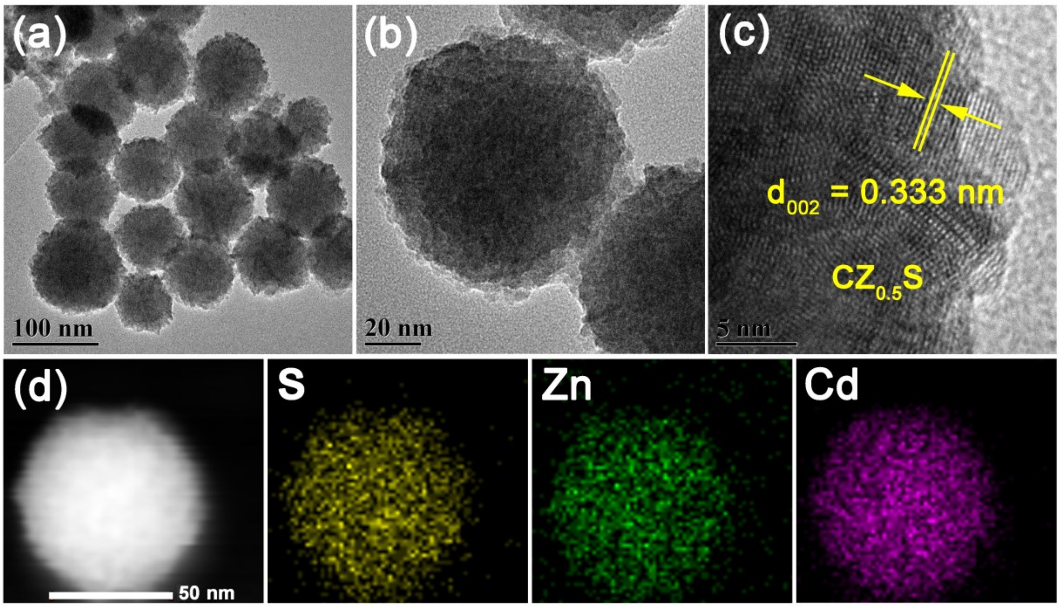

Fig. S2. (a, b) TEM, (c) HRTEM, and (d) dark-field STEM and EDX elemental mapping graphs of $CZ_{0.5}S$ assembled nano-spheres.

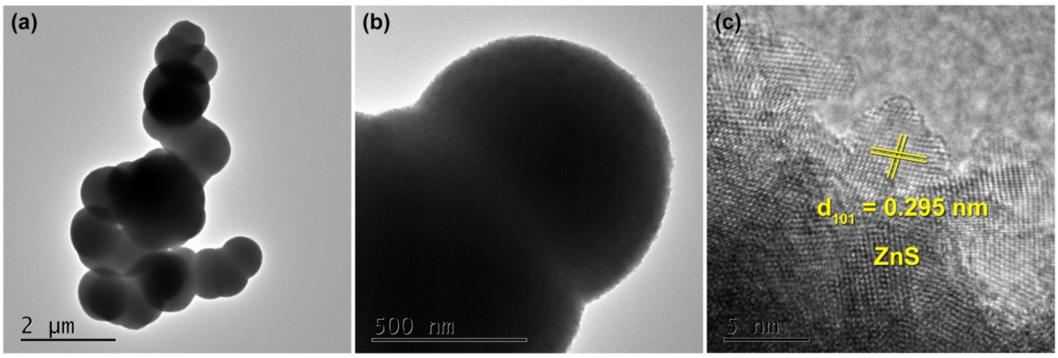

Fig. S3. (a, b) TEM and (c) HRTEM images of ZnS assembled nano-spheres.

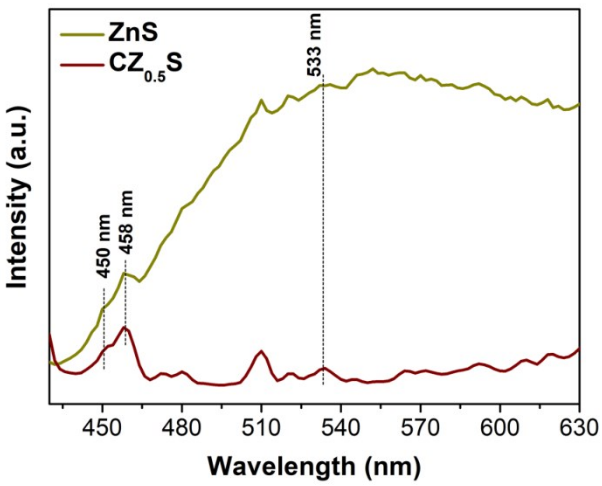

Fig. S4. PL spectra of $CZ_{0.5}S$ and ZnS nano-spheres.

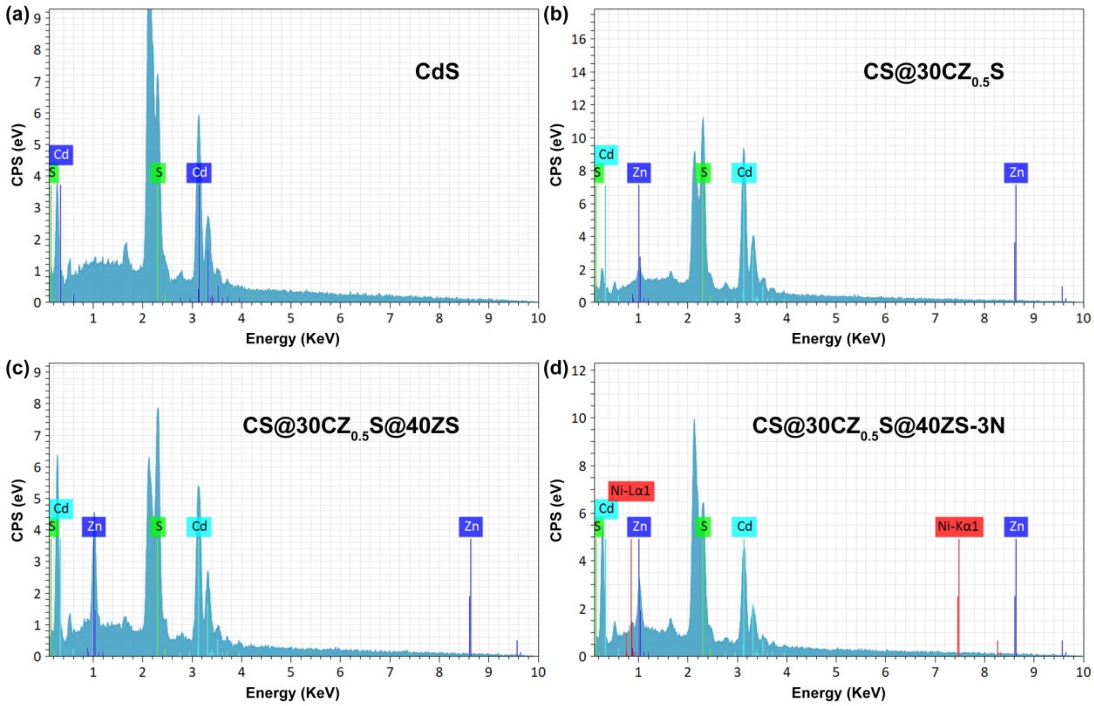

Fig. S5. EDX spectra of (a) CdS, (b) CS@30CZ$_{0.5}$S, (c) CS@30CZ$_{0.5}$S@40ZS, and (d) CS@30CZ$_{0.5}$S@40ZS-3N.

Table S1. The composition of samples determined by EDX measurement.

Catalyst	Cd (at. %)	Zn (at. %)	S (at. %)	Ni (at. %)
CdS	48.21	-	51.79	-
CS@30CZ$_{0.5}$S	45.32	3.71	50.97	-
CS@30CZ$_{0.5}$S@40ZS	34.15	15.32	50.53	-
CS@30CZ$_{0.5}$S@40ZS-3N	35.54	12.67	50.22	1.57

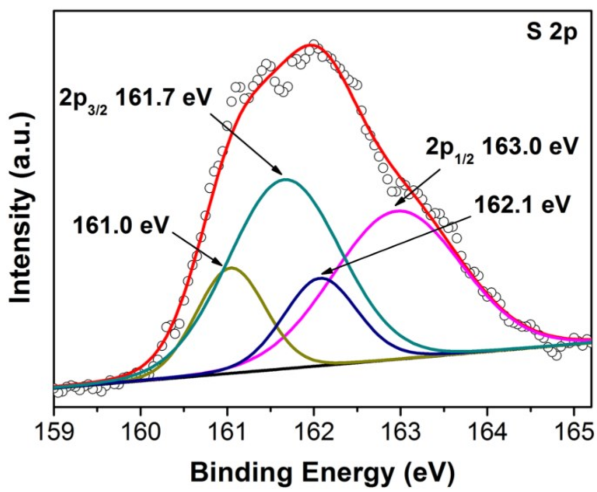

Fig. S6. S 2p XPS spectrum of the CS@30CZ$_{0.5}$S@40ZS-3N hybrid.

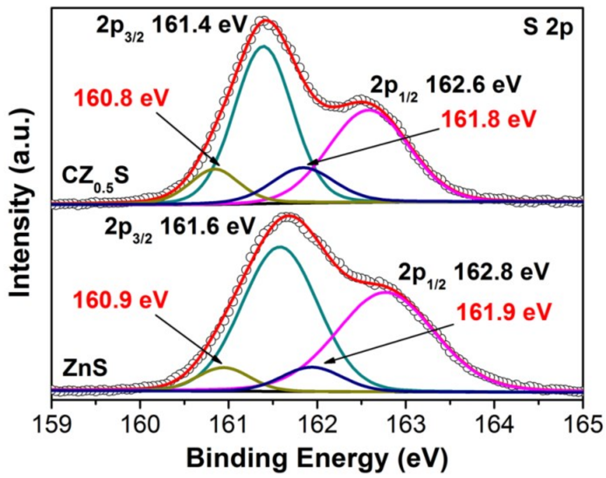

Fig. S7. S 2p XPS spectra of the $CZ_{0.5}S$ and ZnS nano-spheres.

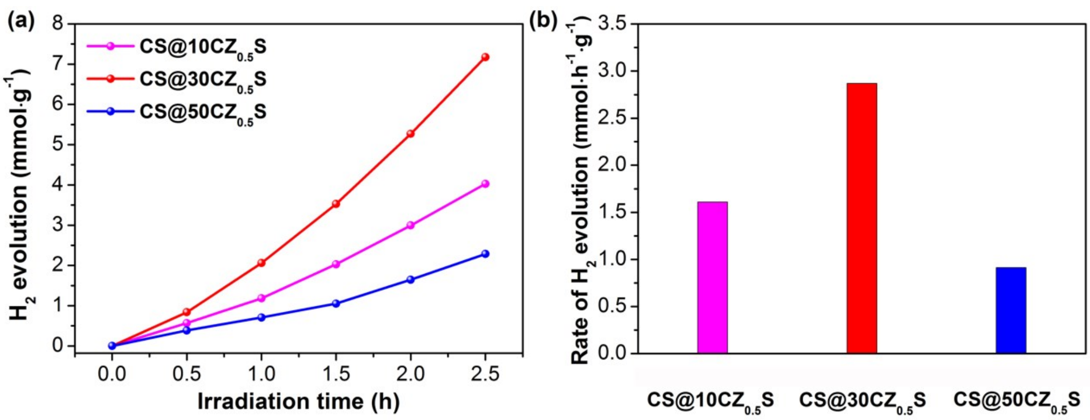

Fig. S8. (a) Photocatalytic HER activities and (b) corresponding rates of the $CdS@CZ_{0.5}S$ composites with different $CZ_{0.5}S$ contents.

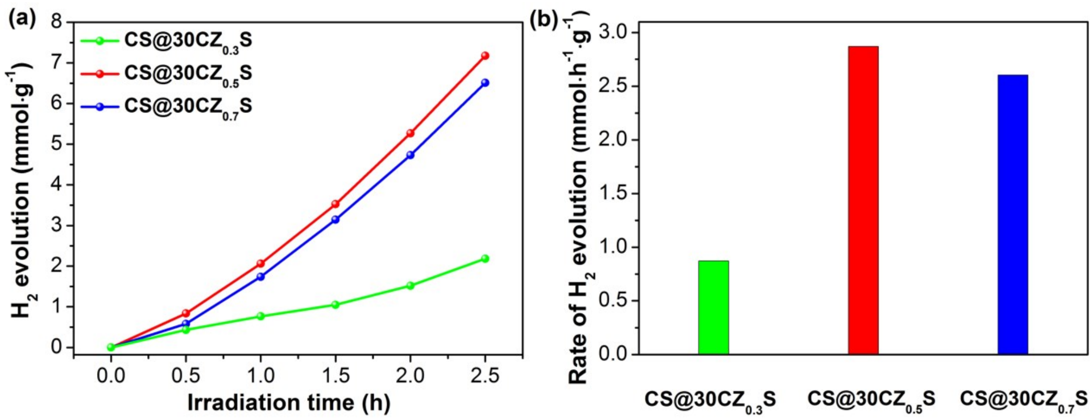

Fig. S9. (a) Photocatalytic H_2 evolution activities and (b) corresponding rates of the CdS@30 wt%$Cd_{1-x}Zn_xS$ with varying Zn ratios in $Cd_{1-x}Zn_xS$.

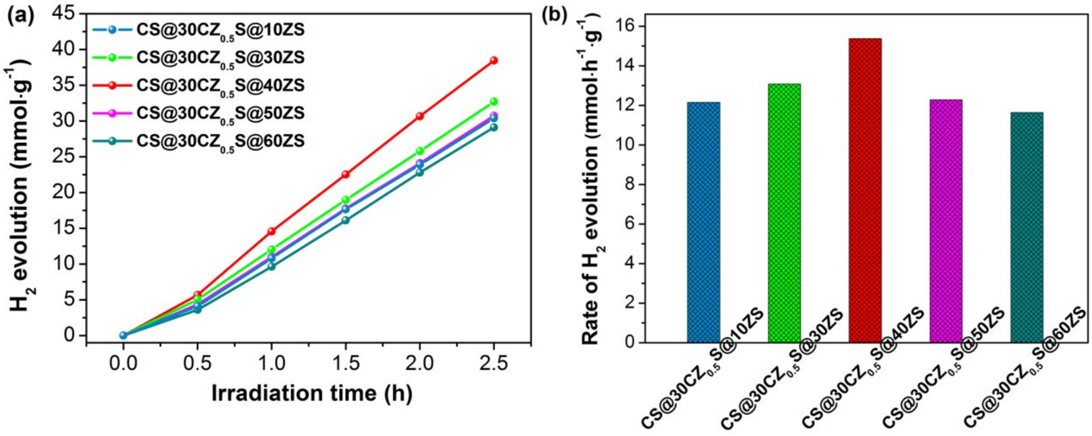

Fig. S10. (a) Photocatalytic HER activities of (b) corresponding rates of the CS@30CZ$_{0.5}$S@ZnS containing different ZnS loading amounts.

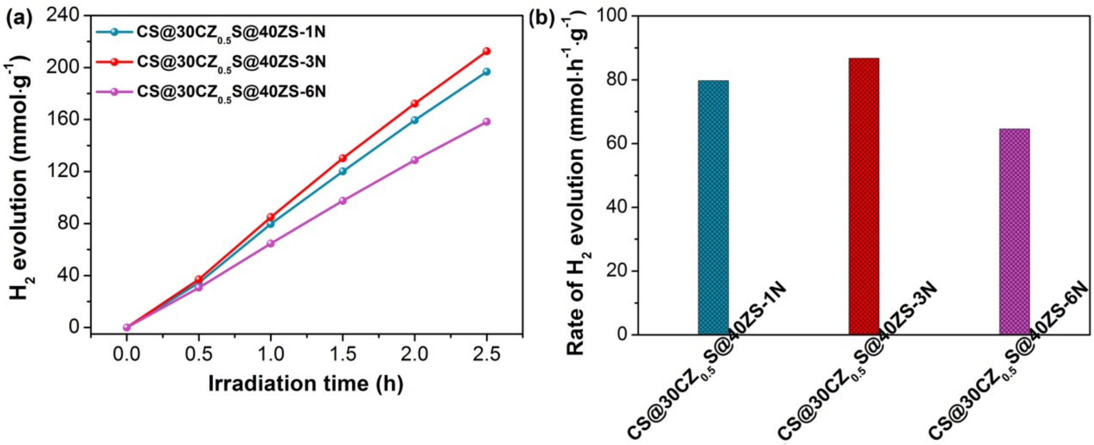

Fig. S11. (a) Photocatalytic HER activities and (b) corresponding rates of the CS@30CZ$_{0.5}$S@40ZS-Ni(OH)$_2$ deposited with different concentrations of Ni(OH)$_2$.

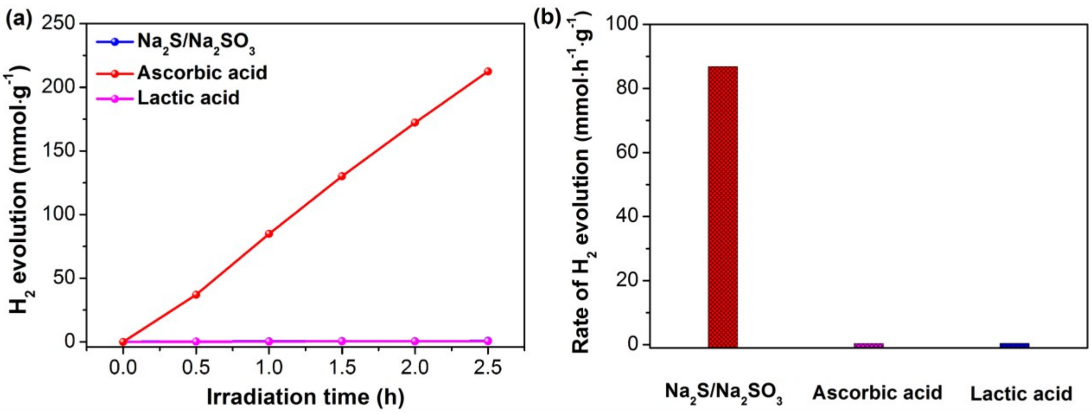

Fig. S12. (a) HER activities and (b) corresponding rates of the Ni-deposited CS@30CZ$_{0.5}$S@40ZS measured employing different hole scavengers.

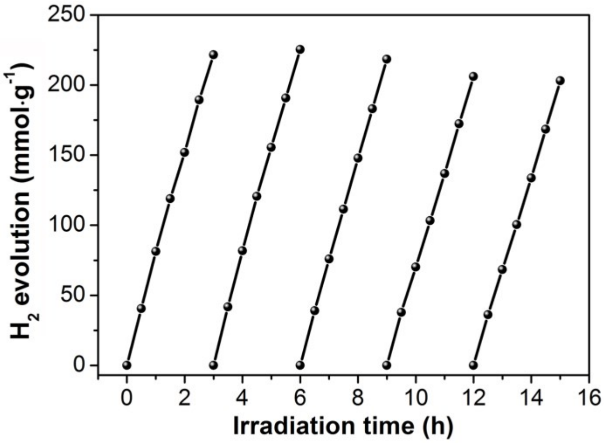

Fig. S13. Cycling HER test for the CS@30C$Z_{0.5}$S@40ZS-3N composite.

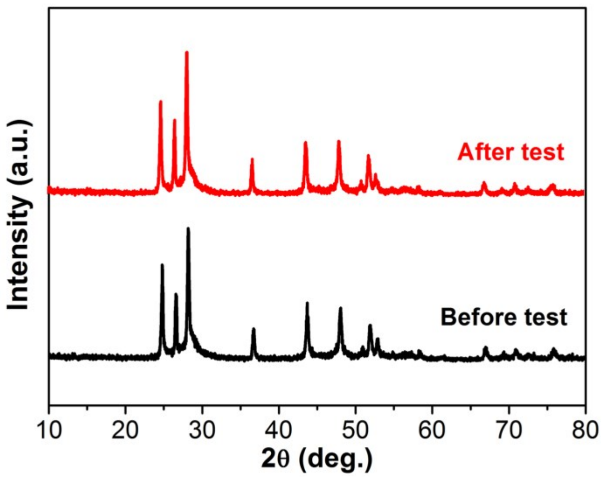

Fig. S14. XRD patterns of the CS@30C$Z_{0.5}$S@40ZS-3N hybrid before and after cycling HER test.

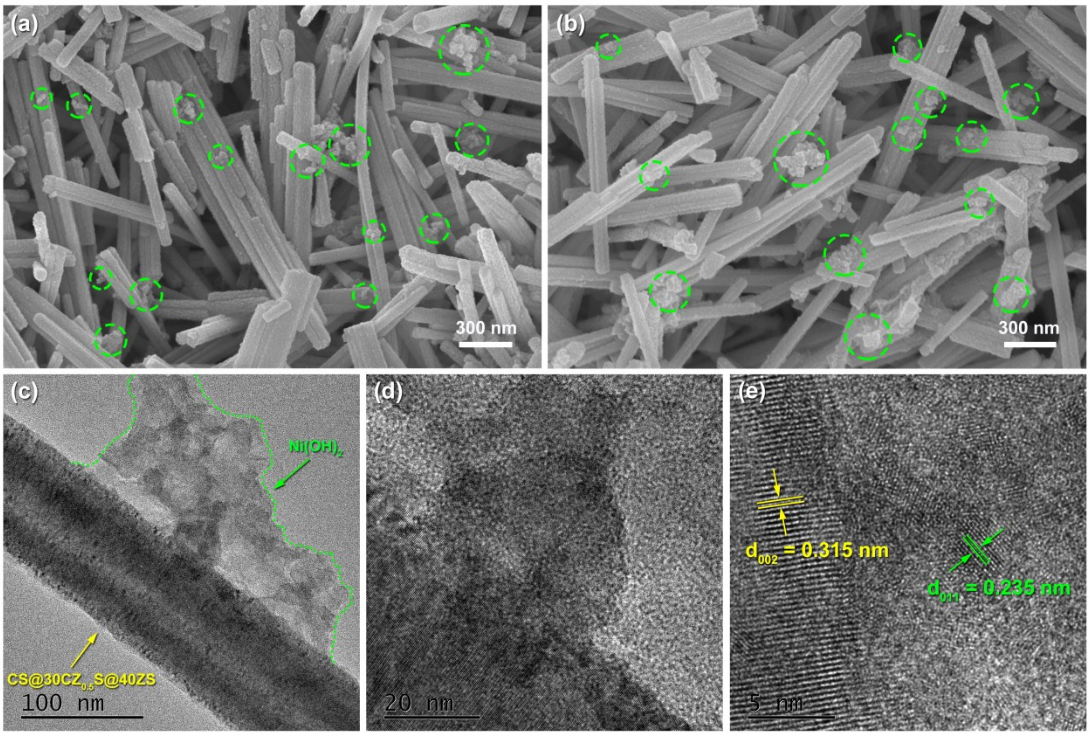

Fig. S15. (a, b) SEM images of the CS@30CZ$_{0.5}$S@40ZS-3N composite (a) before and (b) after cycling activity test. The Ni(OH) was indicated by the green dashed circles. (c, d) TEM and (e) HRTEM photos of the CS@30CZ$_{0.5}$S@40ZS-3N hybrid after the cycling HER measurement.

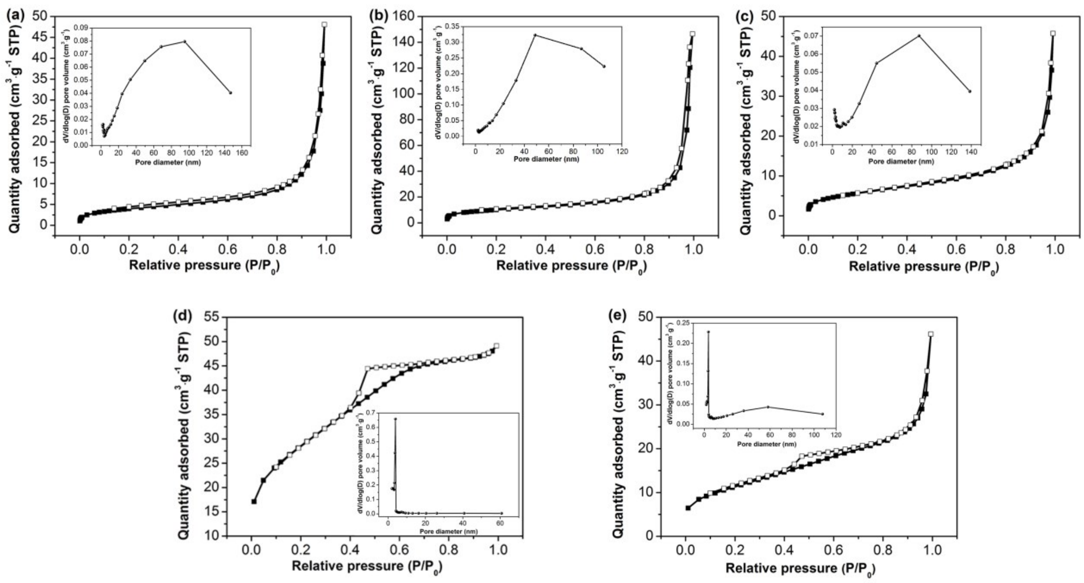

Fig. S16. N_2 adsorption-desorption isotherms and pore-size distributions of (a) CdS, (b) CZ$_{0.5}$S, (c) CS@30CZ$_{0.5}$S, (d) ZnS, and (e) CS@30CZ$_{0.5}$S@40ZS.

Table S2. Comparison on the HER activities of CdS-based photocatalysts.

Photocatalyst	Hole scavenger (aqueous solution)	Light source (Xe lamp)	Maximum rate ($mmol \cdot h^{-1} \cdot g^{-1}$)	AQY (420 nm)	Reference
$CdS@Cd_{0.5}Zn_{0.5}S@ZnS-Ni(OH)_2$	Na_2S/Na_2SO_3	λ > 420 nm	86.79	22.8%	This work
WO_3-Pt-CdS	Na_2S/Na_2SO_3	λ > 420 nm	0.39	-	[1]
$Cd_{1-x}Zn_xS$	Na_2S/Na_2SO_3	λ > 420 nm	46.60	6.56%	[2]
CdS/NiO	Methanol/NaOH	λ > 400 nm	5.91	8.6%	[3]
CdS/ZnS	Na_2S/Na_2SO_3	λ > 420 nm	0.239	16.8%	[4]
Graphene-$Zn_xCd_{1-x}S$	Na_2S/Na_2SO_3	λ > 400 nm	1.06	19.8%	[5]
ZnO/CdS	Na_2S/Na_2SO_3	λ > 400 nm	4.134	-	[6]
CdS/Ni_2O_3	Methanol	λ > 400 nm	4.46	-	[7]
ZnS-(CdS/Pt)	Na_2S/Na_2SO_3	UV-vis light	5.05	-	[8]
$Zn_xCd_{1-x}S/MoS_2$	Na_2S/Na_2SO_3	λ > 420 nm	0.42	-	[9]
$CdS@MoS_2$	Lactic acid	λ > 410 nm	26.14	-	[10]
NiS/CdS	Na_2S/Na_2SO_3	λ > 420 nm	1.13	6.1%	[11]
CdS–ZnS	Na_2S/Na_2SO_3	λ > 420 nm	0.792	-	[12]
$Cu_{1.94}S-Zn_xCd_{1-x}S$	Na_2S/Na_2SO_3	λ > 420 nm	7.74	8.5%	[13]
$Zn_{1-x}Cd_xS$	Na_2S/Na_2SO_3	λ > 420 nm	7.42	9.6%	[14]
$CdS/CdWO_4$	Lactic acid	λ > 420 nm	9.17	-	[15]
$CoO_x/ZnS@CdS/Ni$	Na_2S/Na_2SO_3	λ > 420 nm	20.33	-	[16]
MoS_2/CdS	Lactic acid	λ > 400 nm	3.85	10.5%	[17]
$Cd_{0.5}Zn_{0.5}S$(en)-NiS	Na_2S/Na_2SO_3	λ > 420 nm	38.2	-	[18]
$Ni_2P/Zn_{0.5}Cd_{0.5}S$	Na_2S/Na_2SO_3	λ > 420 nm	22	-	[19]
NiS/CDs/CdS	Na_2S/Na_2SO_3	λ > 420 nm	1.44	-	[20]

Table S3. BET surface areas of different samples.

Catalyst	CdS	$CZ_{0.5}S$	ZnS	$CS@30CZ_{0.5}S$	$CS@30CZ_{0.5}S@40ZS$
S_{BET} ($m^2 \cdot g^{-1}$)	14.37	35.87	100.36	20.72	40.66

References:

[1] M. S. Akple and S. P. Chimmikuttanda, *J. Nanopart. Res.*, 2018, **20**, 231.

[2] J. Song, H. Zhao, R. Sun, X. Li and D. Sun, *Energy Environ. Sci.*, 2017, **10**, 225-235.

[3] X. Chen, W. Chen, H. Gao, Y. Yang and W. Shangguan, *Appl. Catal. B,* 2014, **152-153**, 68-72.

[4] D. Jiang, Z. Sun, H. Jia, D. Lu and P. Du, *J. Mater. Chem. A.*, 2016, **4**, 675-683.

[5] Q. Li, H. Meng, J. Yu, W. Xiao, Y. Zheng and J. Wang, *Chem. Eur. J.*, 2014, **20**, 1176-1185.

[6] S. Wang, B. Zhu, M. Liu, L. Zhang, J. Yu and M. Zhou, *Appl. Catal. B*, 2019, **243**, 19-26.

[7] X. Chen, W. Chen, P. Lin, Y. Yang, H. Gao, J. Yuan and W. Shangguan, *Catal. Commun.*, 2013, **36**, 104-108.

[8] T. Zhuang, Y. Liu, M. Sun, S. Jiang, M. Zhang, X. Wang, Q. Zhang, J. Jiang and S. Yu, *Angew. Chem. Int. Ed.*, 2015, **54**, 11495-11500.

[9] M. Nguyen, P. D. Tran, S. S. Pramana, R. L. Lee, S. K. Batabyal, N. Mathews, L. H. Wong and M. Graetzel, *Nanoscale*, 2013, **5**, 1479-1482.

[10] Y. Yang, Y. Zhang, Z. Fang, L. Zhang, Z. Zheng, Z. Wang, W. Feng, S. Weng, S. Zhang and P. Liu, *ACS Appl. Mater. Interfaces.*, 2017, **9**, 6950-6958.

[11] J. Zhang, S. Qiao, L. Qi and J. Yu, *Phys. Chem. Chem. Phys.,* 2013, **15**, 12088-12094.

[12] Y. Xie, Z. Yu, G. Liu, X. Ma and H. Cheng, *Energy Environ. Sci.*, 2014, **7**, 1895-1901.

[13] Y. Chen, S. Zhao, X. Wang, Q. Peng, R. Lin, Y. Wang, R. Shen, X. Cao, L. Zhang, G. Zhou, J. Li, A. Xia and Y. Li, *J. Am. Chem. Soc.*, 2016, **138**, 4286-4289.

[14] Q. Li, H. Meng, P. Zhou, Y. Zheng, J. Wang, J. Yu and J. Gong, *ACS Catal.*, 2013, **3**, 882-889.

[15] X. Jia, M. Tahir, L. Pan, Z. Huang, X. Zhang, L. Wang and J. Zou, *Appl. Catal., B,* 2016, **198**, 154-161.

[16] L. Zhang, S. Li, B. Liu, D. Wang and T. Xie, *ACS Catal.*, 2014, **4**, 3724-3729.

[17] J. Zhang, Z. Zhu, and X. Feng, *Chem. Eur. J.*, 2014, **20**, 10632-10635.

[18] M. Chen, P. Wu, Y. Zhu, S. Yang, Y. Lu and Z. Lin, *Int. J. Hydrogen Energy.*, 2018, **43**, 10938-10949.

[19] D. Dai, L. Wang, N. Xiao, S. Li, H. Xu, S. Liu, B. Xu, D. Lv, Y. Gao, W. Song, L. Ge and J. Liu, *Appl. Catal., B*, 2018, **233**, 194-201.

[20] R. Wei, Z. Huang, G. Gua, Z. Wang, L. Zeng, Y. Chen and Z. Liu, *Appl. Catal., B*, 2018, **231**, 101-107.